URTeC: 4044071

The Perfect Frac Stage, What's the Value?

Craig Cipolla*[1], Ankush Singh[2], Mark McClure[2], Michael McKimmy[1], John Lassek[1].
1. Hess Corporation, 2. ResFrac Corporation.

This paper was prepared for presentation at the Unconventional Resources Technology Conference held in Houston, Texas, USA, 17-19 June 2024.

Abstract

Real-time fracture treatment optimization has been an aspiration for decades, with modest progress in conventional reservoir tip screen-out designs using rapid mini-frac analysis to adjust pad size and proppant schedules. Real-time treatment optimization in unconventional reservoirs, once thought to be impossible, is now being pursued by operators and service companies. Service companies are automating equipment and enabling "intelligent" completions with low-cost measurements, while operators are envisioning models that can use these low-cost measurements for real-time optimization. However, the value of real-time optimization has not been studied. This paper quantifies the likely value of the perfect frac stage.

The vision of Autonomous and Intelligent Fracturing (AIF) is to enable real-time or stage level improvements in treatment design and/or completion strategy. To realize the AIF vision, there are four major components that are currently missing: (1) fast optimization models, (2) low-cost measurement technologies, (3) reliable fracture geometry control technologies, and (4) the value proposition. This paper introduces the AIF vision and discusses ongoing work to develop fast optimization models and low-cost measurement technologies, but the focus is on the value proposition. Given the operational and subsurface complexities of pad-scale completions and the technology challenges of real-time optimization, we need to understand if such an ambitious goal as AIF is worth the cost. This study focuses on the value of the perfect fracture treatment stage, defined as achieving the design goal of equal fluid and proppant in every cluster.

Two modeling studies were conducted to estimate the value of the perfect frac stage, one using a fully coupled hydraulic fracture-reservoir simulation model and a second study using a simple fracture-reservoir simulation model. The fully coupled model was calibrated using extensive field measurements in the Bakken, including DAS measurements of cluster-level fluid distribution, strain measurements of fracture morphology, fracture propagation pressures from observation lateral gauges, and microseismic measurements of fracture geometry. Both models included five wells and varied well spacing from 440 ft to 1100 ft. Cluster-level fluid distribution was varied from poor to an expected base-case to perfect. The results suggest that well productivity can be improved by as much as 20% if fluid distribution is poor and the perfect stage can be achieved. However, cluster-level fluid distribution may not be "poor" and the perfect frac stage may not be attainable. A conservative estimate for the productivity increases with real-time optimization is discussed in the paper using actual DAS uniformity measurements.

Introduction

Completion optimization is mostly focused on two fronts: (1) evaluation of historical well performance and field trials and (2) data gathering projects using advanced measurement technologies. The combination of field trials and advanced measurements can lead to more reliable models and faster improvements. However, there is still a significant lag between data collection and improvement, presenting an opportunity to add value with more timely decisions. The vision of real-time optimization of hydraulic fracture treatments has been pursued for decades (Cleary et al. 1988, Meyer et al. 1990), but has not been realized. These early attempts at real-time optimization were focused on vertical wells with simple completions; the technical complexities of real-time fracture treatment optimization increase dramatically for multi-stage plug and perf completions typically used in most unconventional reservoirs. Mondal et al. [2022] provide additional historical context.

Fracture treatment pressures are always “monitored” in real-time to ensure safe operations and avoid unwanted screen-outs (Sun et al. 2020). Tip screen-out (TSO) treatment designs are routinely changed in real-time using net pressure behavior and in semi real-time using mini-frac data (Rylance et al. 2023). Ben et al. [2020], Mondal et al. [2022], and Butler et al. [2022] discuss the use of surface pressures to perform specific operational optimizations. However, in most fracture treatments, surface treating pressure does not supply sufficient information to reliably characterize completion effectiveness or fracture geometry. Unfortunately, hydraulic fracture and completion models are not perfect, and measurements of stage-by-stage heterogeneity are not precise or reliable. As a result, relying on real-time “predictions” of fracture geometry and completion effectiveness are not currently possible. In addition, current fracture models capable of capturing the complex behavior of modern plug and perf completions may not provide real-time results. Achieving the vision of real-time optimization is not possible without reliable, low-cost, real-time measurements to calibrate fracture and completion models. Ramakrishnan et al. [2011], Paryani et al. [2018], and Stark et al. [2020, 2024] discuss real-time optimizations, highlighting workflows that integrate measurement technologies.

Automation and control. Another part of real-time optimization is automation and control, enabling optimization models to directly connect and control the fracturing operations. Service companies are continuing to automate fracturing operations and integrate measurement technologies, providing the foundation for AIF. Automating fracture treatment operations should result in more repeatable operations and remove human bias (e.g., rate increase during initial breakdown). The details of these efforts are highlighted on service company websites and marketing materials and are not referenced to avoid commercialism.

Real-time or semi real-time improvements. The final component of AIF is implementing real-time changes or semi real-time changes that materially improve completion effectiveness. Semi real-time improvements could include changes in perforation strategy, stage length, treatment design, and/or cluster spacing. Real-time improvements could use diverters to improve fluid distribution between clusters or alter far-field fracture geometry, adjustments to proppant type or concentration, rate changes, and changes in fluid viscosity. The application of diverters to improve completion effectiveness has been widely evaluated (Quintero et al. 2024, Ajisafe et al. 2024), but is still not routinely applied due to unpredictable results (Murphree et al. 2020). Optimizing limited entry perforation designs has received significant attention and is the primary focus for most operators (Somanchi et al. 2017, Cramer et al. 2019, Horton 2021, Lorwangngam et al. 2023).

The value proposition. There is an important, yet unanswered, question concerning real-time fracture treatment optimization: “what’s the value?” This question also applies to ongoing efforts to optimize completion strategies, including engineered completions (Carpenter 2016) and limited entry perforating. Realizing the vison of AIF and optimizing completion strategies requires considerable time and expense. However, is the expected value worth the investment? In the operator’s area of interest there are insufficient DAS uniformity measurements and corresponding production data to develop a reliable statistical relationship between UI and well productivity. Therefore, to answer this question a detailed modeling study was performed and is the focus of this paper. For context, a summary of the AIF vision is provided before discussing the value of the perfect frac stage.

Autonomous and Intelligent Fracture (AIF)

Butler et al. [2022] introduced the operator's early vision of AIF, presenting a machine learning model that accurately predicted fracture treatment pressures and provided recommendations to improve subsequent stages. **Figure 1** shows the operator's early machine learning model that was successfully assessed in 2021. The data requirements for this early model were fracture treatment design and completion parameters. Semi real-time inputs included rate, treating pressure, proppant concentration, and FR loading.

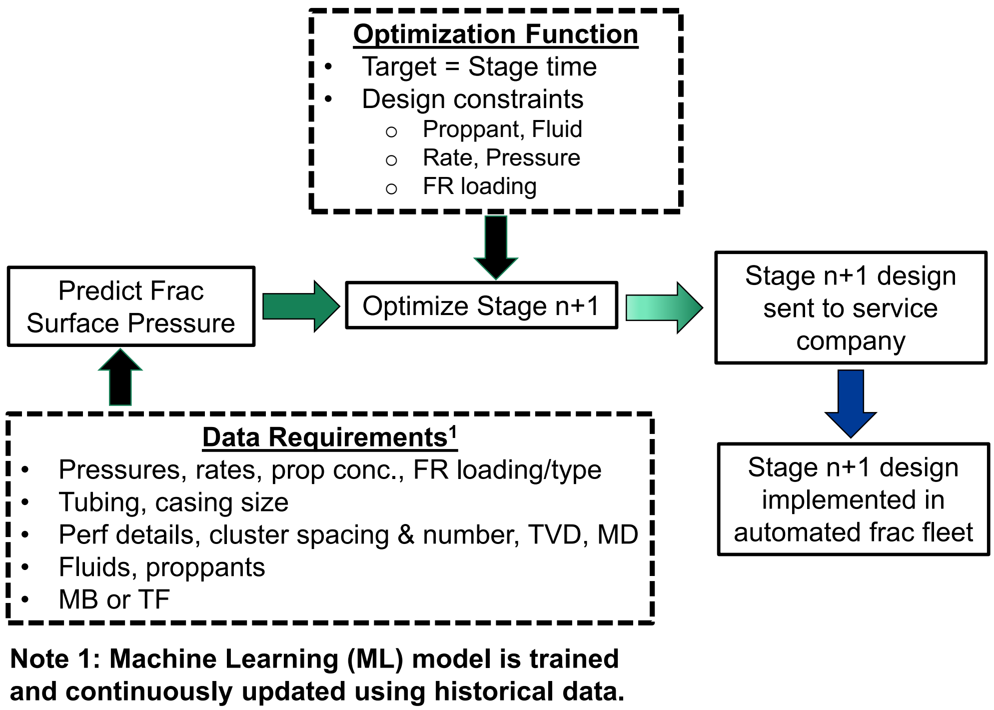

Figure 1 - AIF: Current Capability

The optimization function is simple, providing recommendations to adjust proppant ramp, rate, and FR loading to reduce stage time. However, this simple model did not result in significant improvement when compared to typical recommendations from completion supervisors.

The operator's vision for AIF is shown in **Figure 2**, illustrating the ambitious goal of predicting stage-level production to enable an optimization function that targets value. Realizing this vision requires much more sophisticated and fast models that predict cluster-level fracture geometry. These models require real-time or semi real-time (i.e., after each stage) measurements of fluid and proppant volume injected into each cluster and measurements to constrain fracture length and morphology. Currently, the only reliable real-time measurement of cluster-level fluid and proppant distribution is cemented fiber optics (Ugueto et al. 2015, Somanchi et al. 2017). The most reliable real-time estimates of fracture geometry and morphology are also provided by fiber optics via offset well strain measurement and microseismic (Chen et al. 2022, Cipolla et al. 2022). This highlights two of the four hurdles to achieving the AIF vision:

(1) Low-cost measurement of cluster-level fluid and proppant volume for every stage.
(2) Real-time fracture and production models.

There is ongoing work to develop low-cost measurements that can provide estimates of cluster-level fluid and proppant distribution (Dunham et al. 2023, Cipolla et al. 2024). And there are efforts to correlate offset well pressure behavior to fracture geometry and morphology (Cipolla et al. 2023. Stark et al. 2024). The development of these, or other, low-cost measurements will supply the required real-time model inputs for AIF (Figure 2).

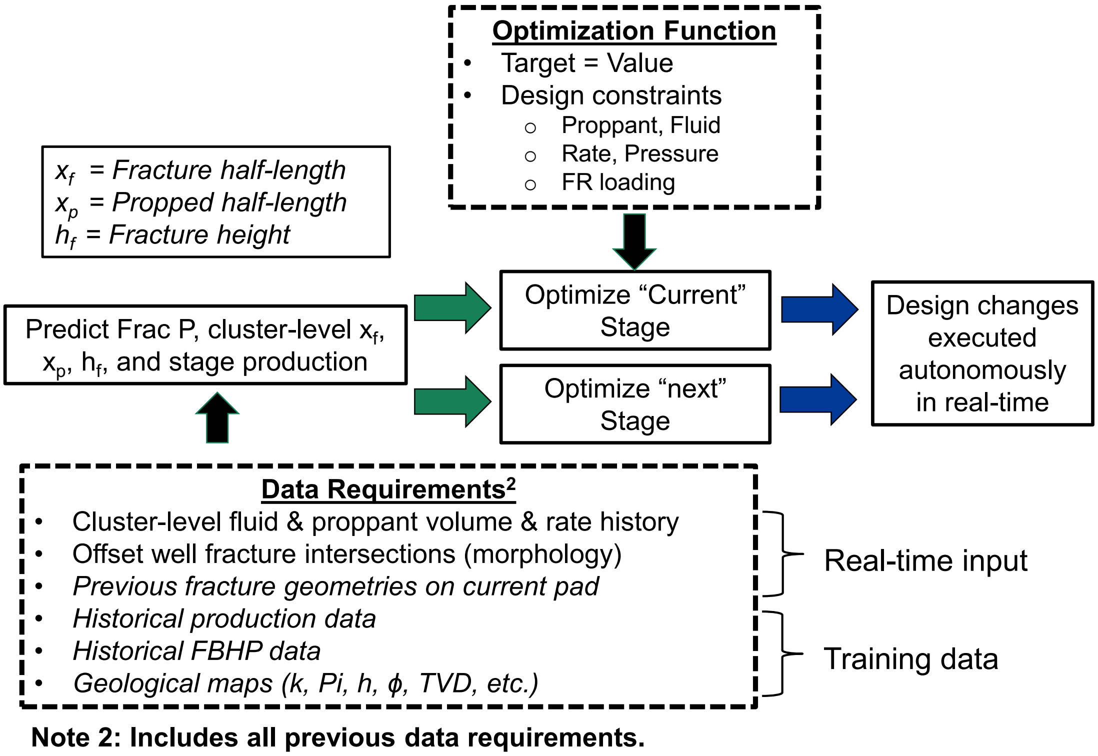

Figure 2 - AIF: The Vision

Fast Fracture Modeling. Without fast hydraulic fracture models, achieving the AIF vision may not be possible. Current efforts focus on using the fracture geometry and morphology measurements in the Bakken (Cipolla et al. 2018, 2020, 2023 and Lorwongngam et al. 2019) to develop simple proxies for fracture geometry and morphology. Although the details of fast fracture modeling are beyond the scope of this paper, a quick summary is provided to introduce this work. **Figure 3** illustrates the measurements and relationships used as inputs to calibrate the fast model. The left side of Figure 3 shows that global fracture length can be predicted using the stage-level fluid volume injected (upper most curve). A simple length-volume relationship was developed using microseismic and fiber optic measurements and represents the average fracture half-length ***for a stage*** as a function of fluid injected (dark green dot). The length of individual fractures in each stage is not known (or measured). However, fracture morphology using offset well fiber-strain data provides measurements of how many fractures are propagated as a function of distance from the wellbore (right graphic in Figure 3, dark red dots represent the average behavior). The center graphic in Figure 3 shows a map view of fracture morphology and asymmetry.

The fracture length-volume and fracture morphology relationships, which can be represented using simple equations or proxies, are combined with a statistical algorithm to match the average behavior and variability of the actual measurements. This global variability is represented by the light green dots in the left-side graphic and light red dots in the right-side graphic. The last component is developing cluster-level length-volume relations for in-zone and out-zone fracture growth. The "relative" difference between in-zone and out-zone fracture growth can be measured, but the length-volume curves are calculated by the algorithm.

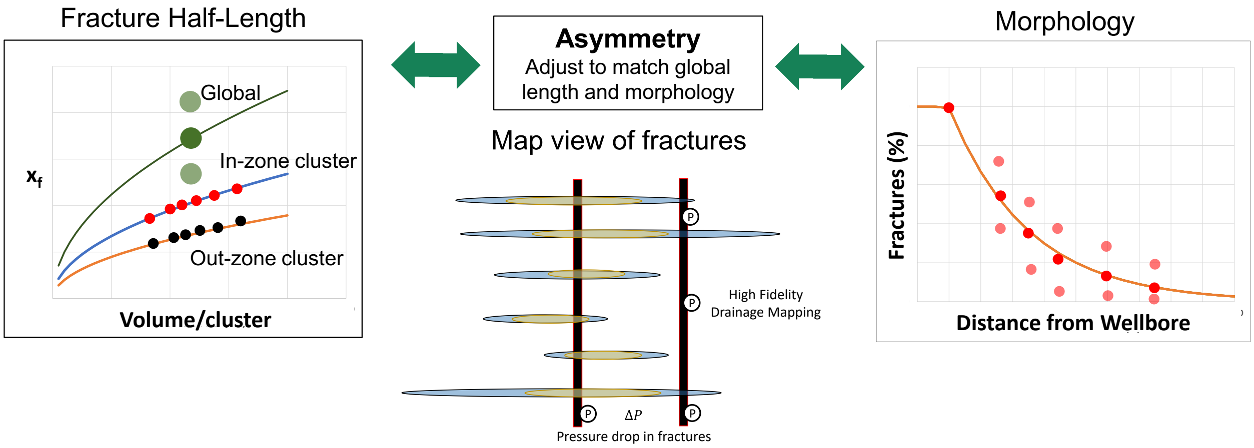

Figure 3 - Fast Fracture Modeling using simple length-volume relations and fracture morphology versus distance.

With inputs of volume injected into each cluster from permanent fiber optics or estimates of stage-level fluid Uniformity Index from surface measurements (Dunham et al. 2023, Cipolla et al. 2024), the model predicts the length of each fracture using the cluster-level in-zone and out-zone curves. This is illustrated in Figure 3 for a six-cluster stage (left graphic, bottom two curves), with different fracture lengths for each cluster predicted using the in-zone (small red dots) and out-zone (small black dots) length-volume curves. The model then uses variations in asymmetry for each fracture to match the morphology behavior (right graphic in Figure 3).

Sufficient cluster-level and stage-level variations in fracture length and asymmetry are introduced by the model to reproduce the variability of the measured data. For example, some stages may have a longer or shorter fracture length than predicted by the global length-volume relationship (light green dots, left graphic in Figure 3), but the well-level average fracture length will honor the global relationship (dark green dot, left graphic in Figure 3). And some stages may have higher or lower morphology than predicted by the average morphology curve (light red dots, right graphic in Figure 3), but the well-level average morphology will honor the global morphology curve (dark red dots, right graphic in Figure 3). Examples of global length-volume and morphology curves are shown in Figures 9 and 12 of SPE 209164 (Cipolla et al. 2022), illustrating the average behavior and variation in measurements. Early versions of the fast frac model are currently being evaluated and work is ongoing to link the frac model to fast production forecasting models.

Uniformity Index and The Perfect Frac Stage

Cluster-level fluid distribution can be determined in real-time using cemented fiber DAS measurements. These measurements are used to evaluate completion effectiveness and typically reported using the Uniformity Index (UI).

(1) $UI = 1 - \sigma/\bar{y}$ where:

σ = standard deviation of cluster-level measurements

$\bar{y}$ = mean of the cluster-level measurements

Figure 4 provides examples of a poor UI and a good UI, showing that fluid distribution can vary considerably from cluster-to-cluster even with a relatively good UI. When UI is poor, some clusters may receive little fluid. **Figure 5** shows the ideal fluid distribution or perfect frac stage, with all clusters receiving the same amount of fluid. Note that the illustrations of UI assume that all clusters breakdown and accept fluid. This is consistent with the operator's DAS, perforation imaging, and proppant tracer data showing that virtually all clusters are being treated, with DAS measurements routinely showing 100% cluster breakdown (Cipolla et al. 2022, Lorwongngam et al. 2023).

A perfectly even distribution of fluid in every cluster may not ensure uniform fracture geometry from each cluster, as stress shadowing will likely result in some degree of non-uniform or asymmetric fracture growth. The left graphic in **Figure 6** illustrates the concept of fracture morphology, where stress shadowing and uneven fluid distribution will result in asymmetric and uneven fracture growth. In each stage, some fractures may propagate much farther in one direction (asymmetry) and some fractures may be much shorter or longer due to nonuniform fluid distribution (low UI). The perfect frac stage, although very unrealistic, would result in uniform fluid distribution and the same fracture geometry in all clusters (right side of Figure 6). The next step is to quantify the value of achieving the perf frac stage.

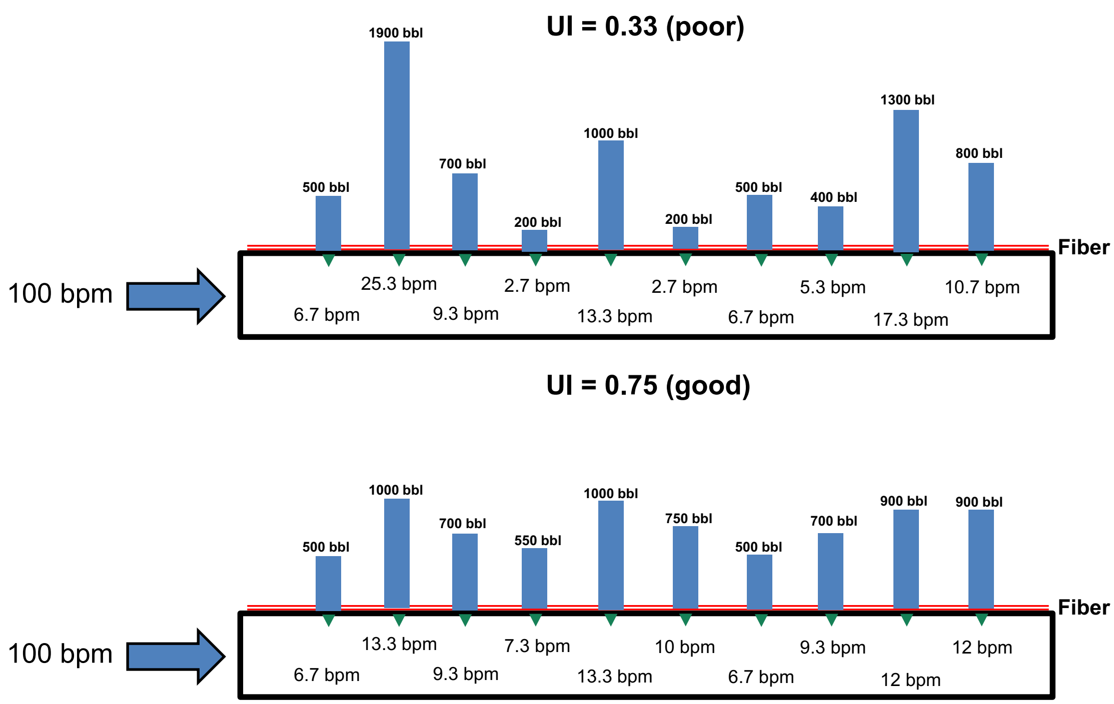

Figure 4 - Illustration of poor UI (top) and good UI (bottom).

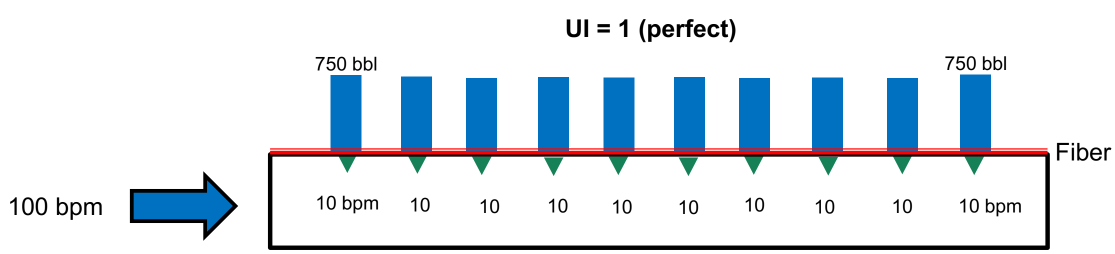

Figure 5 - Illustration of the perfect frac stage.

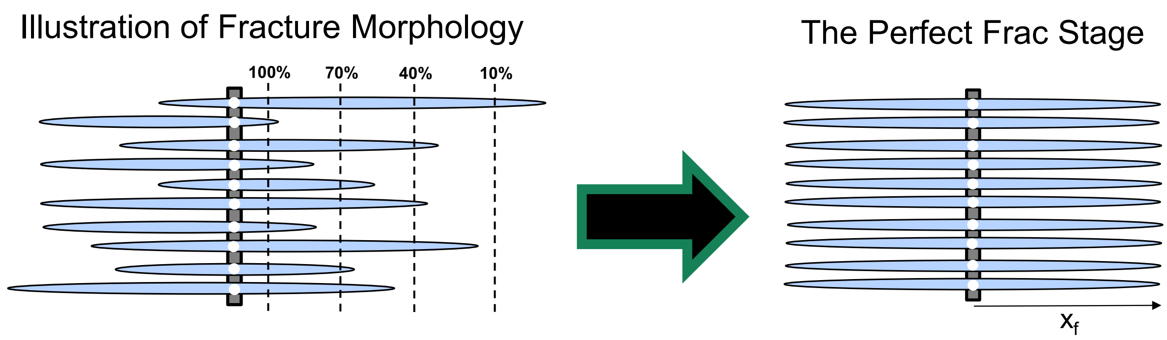

Figure 6 - Fracture morphology and the perfect frac stage

Modeling Study – The Value of the Perfect Frac Stage

The AIF vision is ambitious, requiring substantial time and cost to overcome the three key obstacles previously discussed: (1) fast optimization models, (2) low-cost measurement technologies, and (3) reliable fracture geometry control technologies. The final obstacle is understanding the "size of the prize" to ensure the substantial effort to realize the AIF vision is justified. Two modeling studies were conducted to predict the production improvement and value of the perfect frac stage; one using a fully coupled hydraulic fracture-reservoir simulation model and a second study using the same reservoir simulation model with pre-existing fractures.

The fully coupled hydraulic fracture-reservoir simulation model was calibrated using the comprehensive dataset from the operator's Observation Lateral project (Cipolla et al. 2022). The fracture model accurately reproduced the fracture geometry, morphology, and unique fracture pressure behavior from the observation lateral gauges. The reservoir model was calibrated to match the production history, BHP behavior, and drainage pressures. The fracture and reservoir model calibration process using the operator's loosely coupled model and detailed measurements are illustrated in SPE 209164 (Cipolla et al. 2022). This study used a fully coupled model, but the calibration process was similar. More details of the fully coupled model and the calibration process are provided in **Appendix 1**.

Although the results from the fully coupled model are considered the most realistic, a second study was performed where the hydraulic fracture geometries could be directly input into the same reservoir simulation model. The hydraulic fracture lengths were calculated using a simple fracture model, where fracture length is directly calculated using the cluster-level fluid volume. Fracture conductivity was assumed to be proportional to the cluster-level fluid volume and propped length estimated using a percentage of the total length. The fracture conductivity reduces with effective normal stress. This simple approach resulted in more control of fracture geometry inputs for the reservoir simulations, with the intent of comparing the results from the simple model and fully coupled model to ensure the overall conclusions are not dependent on the details of fracture geometry (e.g., stress shadowing, asymmetry, etc.).

All the models included five Middle Bakken wells and ~1200 ft lateral sectors with 33 ft cluster spacing (36 clusters total). The fully coupled model simulated three stages with 12 clusters per stage. Treatment designs were held constant at 1000 bbls/cluster and 40,000 lbs/cluster using a 50/50 mixture of 100-mesh and 40/70 sand. Four well spacings were modeled to evaluate the impact, if any, of well spacing on the value of the perfect frac stage: 440 ft, 660 ft, 880 ft, and 1100 ft.

Uniformity index. Three different UI cases were modeled, with the base case UI consistent with the operator's DAS measurements showing an average UI of ~0.75 and a standard deviation of 0.09. The standard deviation was used to ensure variations in the model UI were consistent with DAS measurements.

The standard deviation was assumed to be higher when UI is low and, conversely, lower when UI approaches 1. A low-case UI of ~0.25 with a much higher standard deviation of 0.22 was modeled to evaluate the cost of "getting it wrong". This case highlights the cost of poor performance due to problems such as plug failures, crossflow outside the casing due to poor cement, insufficient limited entry, etc. The perfect frac stage was modeled using a UI of 0.95 or higher and standard deviation of 0.04 or lower.

Scenarios are generated with different uniformity index by changing: (a) the random variance in initial perforation diameter, and (b) constants that affect the magnitude of perforation erosion. The near-perfect UI scenario assumes a uniform initial perforation diameter and zero erosion. The modeling assumed that proppant placed in each cluster is proportional to the cluster-level fluid volume. Recent studies show that wellbore proppant transport is a complex process and cluster-level proppant distribution may be significantly different than fluid distribution (Dontsov et al. 2024). The impact of wellbore proppant transport is currently being evaluated and not included in this study.

Fracture geometry and drainage patterns. **Figure 7** shows examples of the fracture geometries (upper graphics) and drainage patterns (lower graphics) predicted by the fully coupled model, illustrating the highly variable fracture lengths and uneven drainage pattern associated with low UI and the more uniform fracture lengths and drainage with the base case UI. The perfect UI case shows very uniform fracture lengths and drainage. The negative effect of low UI on depletion is partially mitigated by well-to-well interaction. Regions with less fracture placement have weaker stress shadowing, making it somewhat more likely that fractures from the adjacent wells will propagate into these regions (See **Appendix 2**).

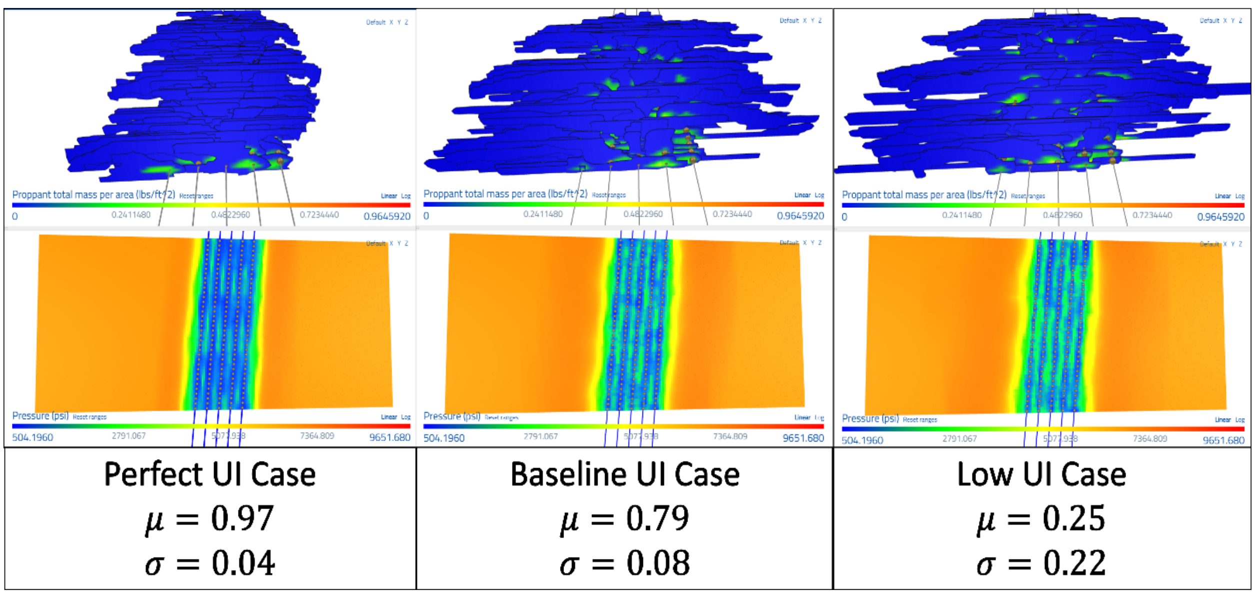

Figure 7 - Fully coupled model results showing fracture geometries (upper graphics) and drainage patterns (lower graphics) for low, base, and perfect UI cases.

Figure 9 shows an example of the input fracture lengths and conductivities used in the simple modeling study. With this simple approach, perfectly uniform fracture lengths and conductivities can be input into the reservoir model. A heel bias in fluid distribution was assumed for the base and low UI cases, resulting in shorter fractures in the toe cluster and longer fractures in the heel clusters. The simple model shows much less heterogeneity in fracture geometry compared to the fully coupled model, which was a goal of the comparison.

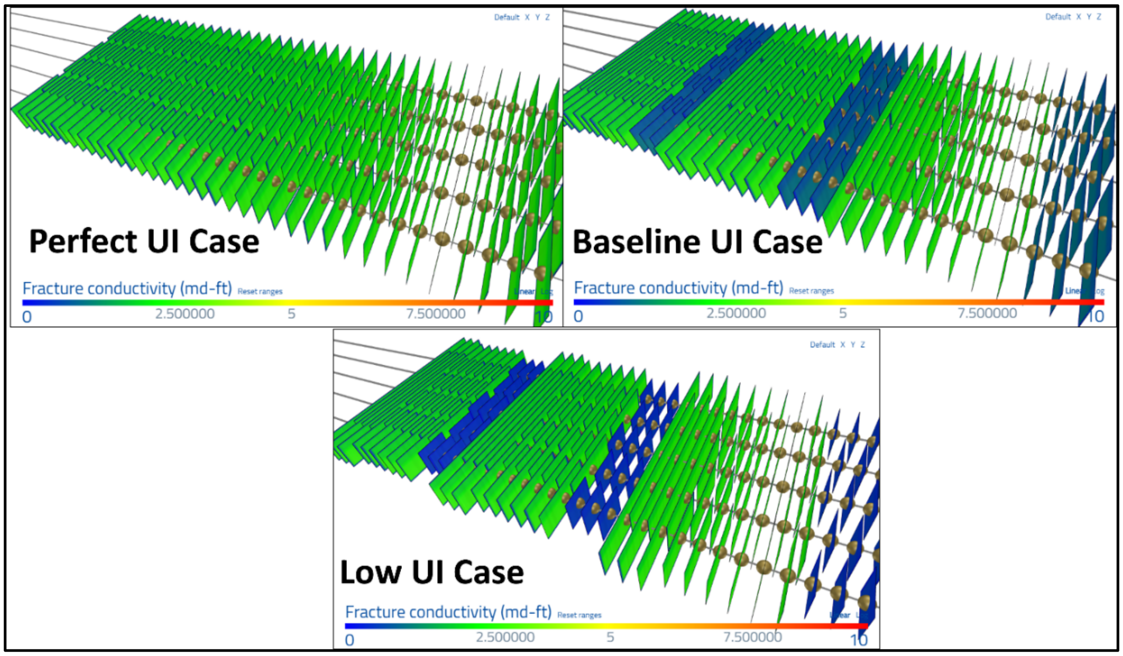

Figure 9 - Example of fracture lengths and conductivity used for the simple model.

Production and economics. **Figure 8** shows the impact of UI on 1-year cumulative production predicted using the fully coupled and simple models (fully coupled model = dots, simple model = triangles). All four well spacings are shown and differentiated by color, but not all symbols are visible due to similarity of results. The production results are presented as a percentage of the base case UI production, with the base case results on the zero % line (y-axis). The UIs for each case in the fully coupled model vary somewhat due to the distribution of parameters used to simulate the different UIs in each model. The UIs for each UI-group in the simple model are the same since they are input parameters. The results from the fully coupled

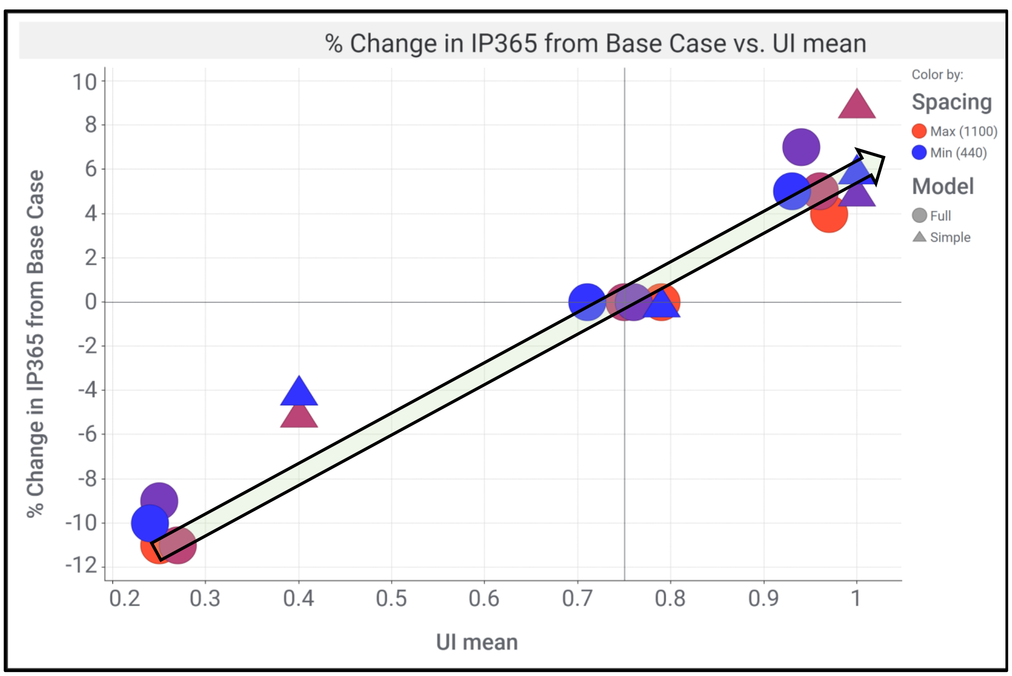

Figure 8 - Impact of UI on 1-year production, simple and fully coupled model.

model and simple model follow the same trend, suggesting the learnings from this work are not dependent on the model. Appendix 2 compares the two modeling results in more detail.

Although the results vary somewhat, the general trend is clear, showing a range in 1-year production of about 20%. If UI can be increased from 0.25 to 0.75, a production increase of 10% in the first year is predicted. The benefits of increasing UI are much less as the average UI improves. First year production increase is about 6% when UI is improved from the base case of 0.75 to almost 1. The benefits of improving UI diminish as production time increases, with the simulations showing an increase of 10% in 10-year cumulative oil when UI is improved from 0.25 to 0.9-1.

The economic impact of variations in UI was estimated using typical Bakken well costs and evaluation parameters. Net present value (NPV) is based on 10-year production. The details of the economic inputs are considered sensitive information, but the results should be representative for Bakken development. **Figure 10** shows the economic impact using the results from the fully coupled model. There is a range of about $2.5 million per well from the low-case UI to the high-case UI (perfect frac stage), while the increase from the base-case (UI=0.75) is about $1 million per well. There are variations in the results for each UI-group due to well spacing, but the trends are consistent. ***Every 0.1 improvement in UI is predicted to increase first year production about 2.5% and add about $0.3 million in NPV***.

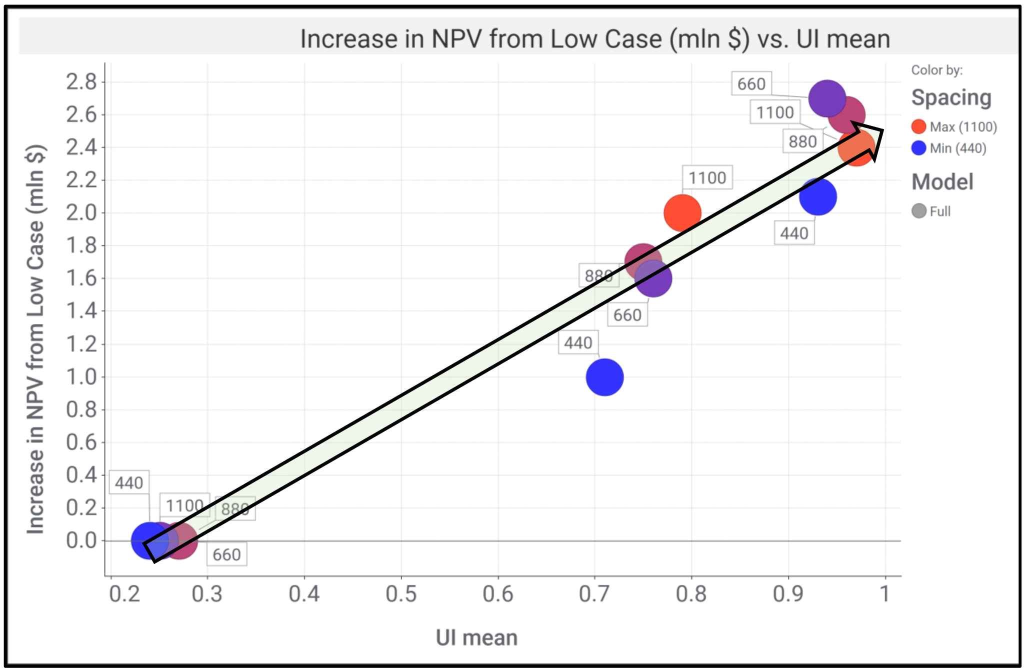

Figure 10 - Incremental Net Present Value, baseline = low case UI

Conclusions - Value of the Perfect Frac Stage

The detailed hydraulic fracture and reservoir simulations show improving UI results in material increases in production and NPV. These simulations do not capture all the benefits of real-time optimization but provide a basis to evaluate the potential value of AIF and ongoing efforts to improve completion effectiveness. Although the modeling is specific to the Bakken, the learnings will likely be applicable when estimating production improvement with increasing UI in other unconventional reservoirs. However, with recent advances in limited entry perforating design, how much opportunity for improvement remains?

The operator's data shows UIs averaging about 0.75 from DAS measurements, suggesting a maximum opportunity for improvement of 0.25 if a UI = 1 could be achieved. However, recent comparisons of DAS measurements and perforation imaging suggest that DAS-measured UIs may be optimistic (Cramer et al.

2024), overpredicting UI by 0.1-0.2. Therefore, it is possible that the operator's UIs could be as low as 0.55 (i.e., 0.2 lower that the DAS average of 0.75), presenting an opportunity to improve UI by 0.45 if a perfect UI could be achieved. Unfortunately, it is unlikely that a perfect UI can be achieved given the complexities of stress shadowing, proppant erosion, etc. Therefore, a UI = 0.9 may be the upper limit, resulting in an opportunity range of 0.15 to 0.35 (current completions = 0.55-0.75 and best cast = 0.9).

If UI can be improved from 0.75 to 0.9, the potential value is about $0.45 million per well. The potential value is over $1 million per well if UI is increased from 0.55 to 0.9. The operator's near-term plan is to drill over 100 wells per year, resulting in a potential value of $45 million per year or more if the AIF vision is realized and UI can be increased. There are still numerous complexities and hurdles to overcome before AIF can be a reality, but continued efforts to advance limited entry designs will likely improve UI and create significant value.

Acknowledgements

The authors would like to thank Hess Corporation for supporting the publication of the work and the Hess Bakken technology team for their support of the AIF project and Fast Frac Model development. Special thanks to Hess Leadership for conceiving, naming, and supporting the AIF vision.

Nomenclature

AIF	*= Autonomous and Intelligent Fracturing*
BHP	*= bottom hole pressure, L2*
bbls	*= barrels, L3*
DAS	*= Distributed Acoustic Sensing*
EUR	*= Estimated Ultimate Recovery*
ft	*= Feet, L*
FR	*= Friction Reducer*
k	*= permeability, L2*
LBS	*= Lower Bakken Shale*
MB	*= Middle Bakken*
md	*= Millidarcy, L2*
MD	*= Measured depth, L*
mln	*= million*
NPV	*= Net present value, $*
p	*= pressure, F/ L2*
Pi	*= initial reservoir pressure, F/L2*
POP	*= Put-on-Production, start of production*
RA	*= radioactive*
STB	*= stock tank barrels, L3*
TF	*= Three Forks*
TSO	*= Tip Screen-out*
TVD	*= True Vertical Depth, L*
UI	*= Uniformity Index*
xf	*= hydraulic fracture half-length, L*
^{o}	*= degrees*
μ	*= average*
ϕ	*= porosity*
σ	*= standard deviation*
$\bar{y}$	*= mean*

SI Metric Conversion Factors

acre	x	4.046 873e+03	=	m^2
bbl	x	1.589 874e-01	=	m^3
cp	x	1.0e-03	=	Pa.s
ft	x	3.048e-01	=	m
°F		(°F – 32)/1.8	=	°C
lbm/gal	x	1.198 264e+02	=	kg/cm^2
psi	x	6.894 757e+00	=	kPa

References

Ajisafe, F. O., Porter, H., Kothare, S., Colson, E., Ellis, R., Heaton, N., Demars, B., and M. Mayerhofer. "Protecting Parent-Well Production Using Far-Field Diverters in Unconventional Wells." Paper presented at the SPE Hydraulic Fracturing Technology Conference and Exhibition, The Woodlands, Texas, USA, February 2024. doi: https://doi.org/10.2118/217813-MS.

Ben, Yuxing , Perrotte, Michael , Ezzatabadipour, Mohammadmehdi , Ali, Irfan , Sankaran, Sathish , Harlin, Clayton, and Dingzhou Cao. "Real-Time Hydraulic Fracturing Pressure Prediction with Machine Learning." Paper presented at the SPE Hydraulic Fracturing Technology Conference and Exhibition, The Woodlands, Texas, USA, February 2020. doi: https://doi.org/10.2118/199699-MS.

Butler, Erin, Pertuso, Dryonis, Hua, Gerald, and Price Stark. "Automated Hydraulic Fracturing Integrated with Predictive Machine Learning." Paper presented at the SPE Hydraulic Fracturing Technology Conference and Exhibition, The Woodlands, Texas, USA, February 2022. doi: https://doi.org/10.2118/209165-MS.

Carpenter, Chris. "Engineered Shale Completions Based on Common Drilling Data." J Pet Technol 68 (2016): 86–88. doi: https://doi.org/10.2118/0916-0086-JPT.

Chen, Mengyuan, Tang, Jin, Zhu, Ding, and Alfred Hill. "Classification and Localization of Fracture-Hit Events in Low-Frequency Distributed Acoustic Sensing Strain Rate with Convolutional Neural Networks." SPE J. 27 (2022): 1341–1353. doi: https://doi.org/10.2118/205136-PA.

Cipolla, C., Motiee, M., and Kechemir, A. 2018. Integrating Microseismic, Geomechanics, Hydraulic Fracture Modeling, and Reservoir Simulation to Characterize Parent Well Depletion and Infill Well Performance in the Bakken. Paper presented at the Unconventional Resources Technology Conference held in Houston, Texas, USA, 23–25 July 2018. URTeC 2899721. https://doi.org/10.15530/URTEC-2018-2899721.

Cipolla, C., Litvak, M., Prasad, S., McClure, M. 2020 Case History of Drainage Mapping and Effective Fracture Length in the Bakken. Paper presented at the SPE Hydraulic Fracture Technical Conference and Exhibition, The Woodlands, Texas, USA, 4-6 February. SPE 199716-MS. https://doi.org/10.2118/199716-MS.

Cipolla, C., Wolters, J., McKimmy, M., Miranda, C., Hari-Roy, S., Kechemir, A., Gupta, N. 2022. Observation Lateral Project: Direct Measurement of Far-field Drainage. Paper presented at SPE Hydraulic Fracturing Technology Conference and Exhibition, The Woodlands, Texas, USA, February 2022. SPE-209164-MS. https://doi.org/10.2118/209164-PA

Cipolla, Craig, McKimmy, Michael, Hari-Roy, Stephanie, Wolters, Jennifer, Haffener, Jackson, Haustveit, Kyle, and Mouin Almasoodi. "Evaluating Stimulation Effectiveness with Permanent Optical Fiber and Sealed Wellbore Pressure Monitoring: Bakken Shale Case Study." SPE Drill & Compl 38 (2023): 146–154. doi: https://doi.org/10.2118/209129-PA.

Cipolla, C., McKimmy, M., Lassek, J., Fatheree, K., Aghdam, S., Kroschel, J., and Khan, M. 2024. Case Study - Using an Acoustically Derived Surface Metric to Approximate Fluid Distribution Uniformity During Stimulation. Paper presented at the Unconventional Resources Technology Conference held in Houston, Texas, USA, 17–19 June 2024. URTeC 4044703.

Cleary, M. P., Barr, D. T., and R. M. Willis. "Enhancement of Real-Time Hydraulic Fracturing Models with Full 3-D Simulation." Paper presented at the SPE Gas Technology Symposium, Dallas, Texas, June 1988. doi: https://doi.org/10.2118/17713-MS.

Cramer, David , Friehauf, Kyle , Roberts, Glyn , and Jeff Whittaker. "Integrating DAS, Treatment Pressure Analysis and Video-Based Perforation Imaging to Evaluate Limited Entry Treatment Effectiveness." Paper presented at the SPE Hydraulic Fracturing Technology Conference and Exhibition, The Woodlands, Texas, USA, February 2019. doi: https://doi.org/10.2118/194334-MS.

Cramer, David, and Kyle Friehauf. "Methods for Assessing Proppant Coverage Along the Lateral for Plug-And-Perf Treatments." Paper presented at the SPE Hydraulic Fracturing Technology Conference and Exhibition, The Woodlands, Texas, USA, February 2024. doi: https://doi.org/10.2118/217778-MS.

Dontsov, Egor, Hewson, Christopher, and Mark McClure. "A New Crack Propagation Algorithm That Enables Accurate Simulation of Propagation Across Thin Layers in a Practical Field-Scale Fracturing Model." Paper presented at the SPE Hydraulic Fracturing Technology Conference and Exhibition, The Woodlands, Texas, USA, February 2022. doi: https://doi.org/10.2118/209146-MS.

Dontsov, Egor, Ponners, Christopher, Torbert, Kevin, and Mark McClure. "Practical Optimization of Perforation Design with a General Correlation for Proppant and Slurry Transport from the Wellbore." Paper presented at the SPE Hydraulic Fracturing Technology Conference and Exhibition, The Woodlands, Texas, USA, February 2024. doi: https://doi.org/10.2118/217771-MS.

Dunham, Eric M., Zhang, Junwei, and Dan Moos. "Constraints on Pipe Friction and Perforation Cluster Efficiency from Water Hammer Analysis." Paper presented at the SPE Hydraulic Fracturing Technology Conference and Exhibition, The Woodlands, Texas, USA, January 2023. doi: https://doi.org/10.2118/212337-MS.

Horton, Blake "A Shot in the Dark: How Your Post-Fracture Perforation Imaging can be Misleading and How to Better Understand Cluster Efficiency and Optimize Limited Entry Perforating." Paper presented at the SPE Hydraulic Fracturing Technology Conference and Exhibition, Virtual, May 2021. doi: https://doi.org/10.2118/204177-MS.

Lorwongngam, A., Cipolla, C., Gradl, G. et al. 2019. Multidisciplinary Data Gathering to Characterize Hydraulic Fracture Performance and Evaluate Well Spacing in the Bakken. Paper presented at the SPE Hydraulic Fracturing Technology Conference held in The Woodlands, Texas, USA, 5–7 February 2019. SPE-194321-MS. https://doi.org/10.2118/194321-MS.

Lorwongngam, Apiwat Ohm, McKimmy, Michael, Oughton, Evan, and Craig Cipolla. "One Shot Wonder XLE Design: A Continuous Improvement Case Study of Developing XLE Design in the Bakken." Paper presented at the SPE Hydraulic Fracturing Technology Conference and Exhibition, The Woodlands, Texas, USA, January 2023. doi: https://doi.org/10.2118/212358-MS.

Machado, Thiago, and Adnan Mohammed. "AI in Hydraulic Fracturing: The Journey from Guessing to Certainty." Paper presented at the SPE Symposium Leveraging Artificial Intelligence to Shape the Future of the Energy Industry, Al Khobar, Saudi Arabia, January 2023. doi: https://doi.org/10.2118/214463-MS.

McClure, M., Kang, C., Hewson, C., Medam, S., Dontsov, E., and Singh, A. ResFrac Technical Writeup. 2023. http://arxiv.org/abs/1804.02092.

McKimmy, M., Hari-Roy, S., Cipolla, C., Wolters, J., Haffener, J., Haustveit, K., 2022. Hydraulic Fracture Geometry, Morphology, and Parent-Child Interactions: Bakken Case Study. SPE 209162. Presented at the SPE Hydraulic Fracturing Technology Conference and Exhibition held 1-3 February 2022, in The Woodlands, Texas, USA. https://doi.org/10.2118/209162-MS.

Meyer, B. R., Cooper, G. D., and S. G. Nelson. "Real-Time 3-D Hydraulic Fracturing Simulation: Theory and Field Case Studies." Paper presented at the SPE Annual Technical Conference and Exhibition, New Orleans, Louisiana, September 1990. doi: https://doi.org/10.2118/20658-MS.

Mondal, Somnath, Garusinghe, Ashan, Ziman, Sebastian, Abdul-Hameed, Muhammed, Paleja, Rakesh, Jones, Matthew, Limbeck, Jan, Bartmann, Bryce, Young, Jeremy, Shanley, Kent, Cardwell, Bonner, Klobodu, Humphrey, Huckabee, Paul, Ugueto, Gustavo, and Christopher Ledet. "Efficiency and Effectiveness - A Fine Balance: An Integrated System to Improve Decisions in Real-Time Hydraulic Fracturing Operations." Paper presented at the SPE Hydraulic Fracturing Technology Conference and Exhibition, The Woodlands, Texas, USA, February 2022. doi: https://doi.org/10.2118/209127-MS.

Murphree, Chase , Kintzing, Malcolm , Robinson, Stephen , and Jay Sepehri. "Evaluating Limited Entry Perforating & Diverter Completion Techniques with Ultrasonic Perforation Imaging & Fiber Optic DTS Warmbacks." Paper presented at the SPE Hydraulic Fracturing Technology Conference and Exhibition, The Woodlands, Texas, USA, February 2020. doi: https://doi.org/10.2118/199712-MS.

Paryani, Mohit , Sia, Djamel , Mistry, Bhavina , Fairchild, Drew , and Ahmed Ouenes. "Real-Time Completion Optimization of Fracture Treatment Using Commonly Available Surface Drilling and Fracing Data." Paper presented at the SPE Canada Unconventional Resources Conference, Calgary, Alberta, Canada, March 2018. doi: https://doi.org/10.2118/189810-MS.

Quintero, A., Sepúlveda, E., Reina, J., and J. Bahamón. "Enhanced Injectivity Using Diversion Technology on Hydraulic Fracturing Jobs in Los Llanos Basin." Paper presented at the SPE International Conference and Exhibition on Formation Damage Control, Lafayette, Louisiana, USA, February 2024. doi: https://doi.org/10.2118/217907-MS.

Ramakrishnan, H.. , Yuyan, Rioka , and J.. Belhadi. "Real-Time Completion Optimization Of Multiple Laterals In Gas Shale Reservoirs: Integration of Geology, Log, Surface Seismic, and Microseismic Information." Paper presented at the SPE Hydraulic Fracturing Technology Conference, The Woodlands, Texas, USA, January 2011. doi: https://doi.org/10.2118/140542-MS.

Rylance, Martin, Kogsbøll, Hans-Henrik, Cipolla, Craig, Montgomery, Carl T., Smith, Michael B., Norman, W. David, Olson, Karen E., and C. Mark Pearson. "Tip Screen Out Fracturing Delivering Optimum Performance in Conventional Applications for 40 Years: Case Histories and Lessons Learned." Paper presented at the SPE Hydraulic Fracturing Technology Conference and Exhibition, The Woodlands, Texas, USA, January 2023. doi: https://doi.org/10.2118/212365-MS.

Somanchi, Kiran , Brewer, James , and Alan Reynolds. "Extreme Limited Entry Design Improves Distribution Efficiency in Plug-n-Perf Completions: Insights from Fiber-Optic Diagnostics." Paper presented at the SPE Hydraulic Fracturing Technology Conference and Exhibition, The Woodlands, Texas, USA, January 2017. doi: https://doi.org/10.2118/184834-MS.

Sun, Jianlei John, Battula, Arvind, Hruby, Brandon, and Paymon Hossaini. "Application of Both Physics-Based and Data-Driven Techniques for Real-Time Screen-Out Prediction with High Frequency Data." Paper presented at the SPE/AAPG/SEG Unconventional Resources Technology Conference, Virtual, July 2020. doi: https://doi.org/10.15530/urtec-2020-3349.

Stark, Price , Tran, John-Bosco , Mogck, Drew , and Gene Mask. "Improving Completions Immediately: An Applied Methodology for Real-Time Optimization." Paper presented at the SPE Hydraulic Fracturing Technology Conference and Exhibition, The Woodlands, Texas, USA, February 2020. doi: https://doi.org/10.2118/199698-MS.

Stark, Price, Adil, Faraaz, Woodward, Beau, Treviño, Julio, Steinhoff, Chris, and Dana Gallegos. "Real-time Awareness: A Novel Application of Fiber Optics to Optimize Simultaneous Operations of Drilling and Frac." Paper presented at the SPE Hydraulic Fracturing Technology Conference and Exhibition, The Woodlands, Texas, USA, February 2024. doi: https://doi.org/10.2118/217777-MS.

Ugueto C., Gustavo A., Huckabee, Paul T., Molenaar, Mathieu M., Wyker, Brendan , and Kiran Somanchi. "Perforation Cluster Efficiency of Cemented Plug and Perf Limited Entry Completions; Insights from Fiber Optics Diagnostics." Paper presented at the SPE Hydraulic Fracturing Technology Conference, The Woodlands, Texas, USA, February 2016. doi: https://doi.org/10.2118/179124-MS.

Appendix 1 - Details of the Numerical Simulator and Model Calibration

The simulations are performed with a combined hydraulic fracturing, wellbore, and reservoir simulator (McClure et al., 2023). In every timestep, the simulator solves: (a) mass balance on fluid components (water, oil, and gas, when using the black oil model), water solute components (such as friction reducer), and user-defined proppant types; (b) fracture mechanics equations for propagation and stress shadowing; (c) poroelastic stress changes from pore pressure changes in the matrix; and (d) momentum balance in the wellbore elements. The simulator is a 'true' hydraulic fracturing simulator, in the sense that it meshes cracks as cracks and incorporates realistic equations for proppant transport and fracture opening and closure. The fracture mesh is nonconforming to the global matrix mesh. A local grid refinement technique is used to capture fluid exchange between the fracture and matrix elements (Section 2.3 from McClure et al., 2023). To increase resolution and accuracy, the simulator tracks the position of the crack-tip within each fracture element, using the technique developed by Dontsov et al. [2022].

Model calibration. A model was built and calibrated based on the observation lateral pad described by Cipolla et al. [2022]. The history match is based on (**Figure 11**): (a) Cluster efficiency from fiber and downhole camera observations, (b) Production volumes, oil rates, water cut and GOR for parent and child wells. Production performance between the wells based on vintage and position was also matched, (c)

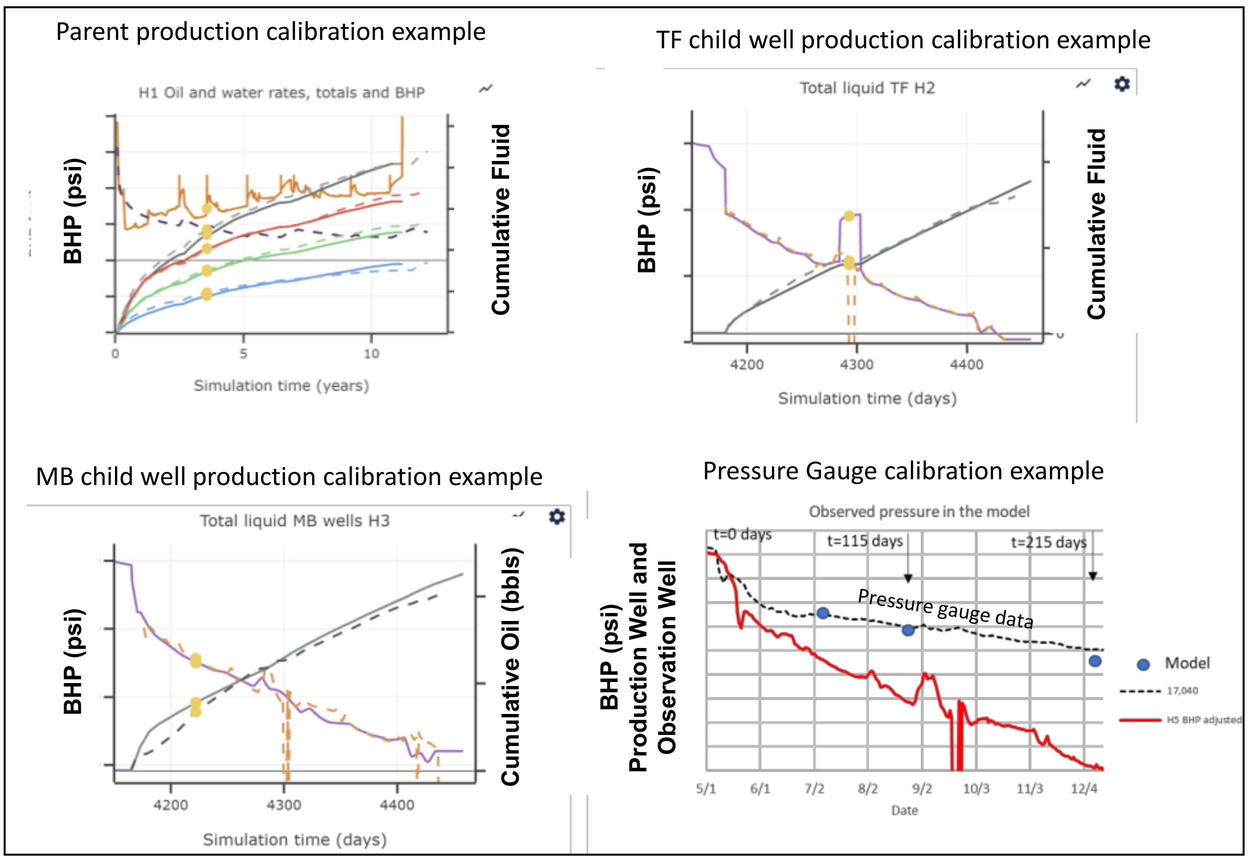

Figure 11 - Examples from the observation lateral model calibration.

Changes in production rates in the parent well caused by frac hits from the children wells, (d) Fracture morphology parameters including dimensions based on fiber and microseismic, volume to first response based on fiber observations and facture net pressure from cemented downhole pressure gauge observations during the stimulation, (e) Far-field depletion from offset pressure gauges, (f) Pressure communication at POP was calibrated to the interference tests.

Appendix 2 – Simple and Fully Couple Model: Comparing Results

This appendix provides more details and examples comparing the fully coupled and simple models. As discussed, the intent of the two-model approach was to ensure that the conclusions from this study were not unduly dependent on the modeling approach.

Utilizing the parameters from the calibrated model, the generic five-well model was set up as a base case simulation for the sensitivity analysis. The simulations include both fracturing and production. **Figure 12** shows results from the baseline scenario. Stress shadowing causes the fracture geometry to be variable and asymmetric even in the case with the perfect UI. This fracture morphology is realistic and has been calibrated to match the timing and quantity of frac hits in the offset wells. In addition, stress shadowing balances with limited-entry pressure drop to determine the perforation efficiency.

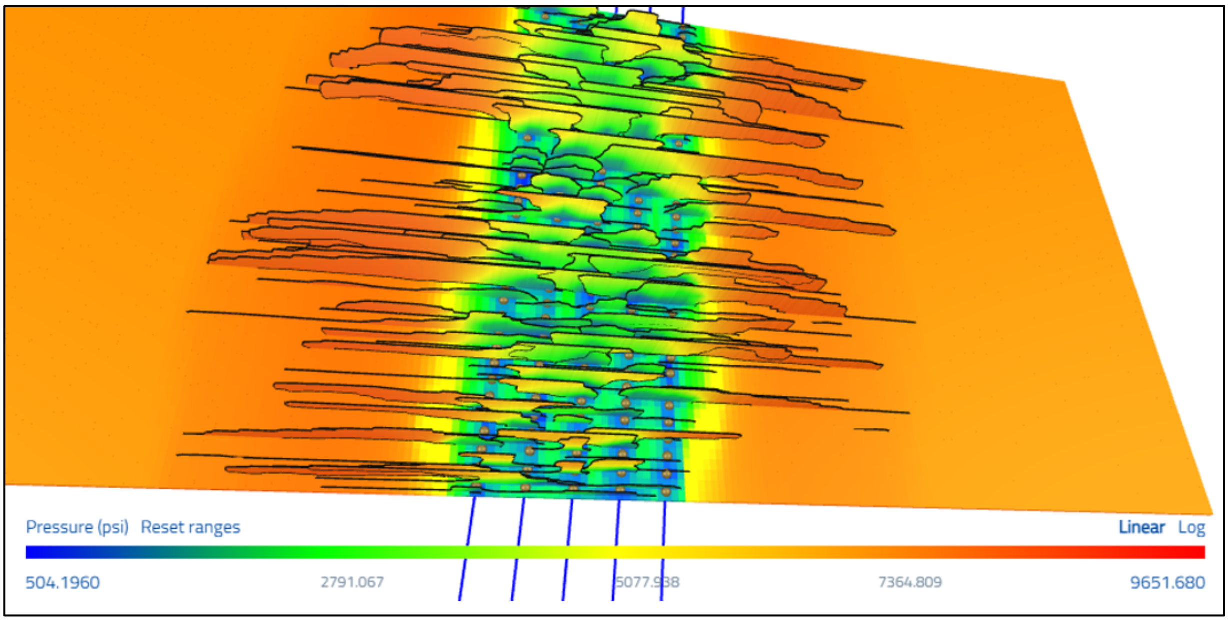

Figure 12 - Fully coupled model, baseline scenario, using observation lateral calibrated model parameters.

For additional sensitivity analysis, simulations were run with an idealized geometry. These models assume symmetric, rectangular fractures. Fracture length is determined from fluid allocations using a simple power law function and propped length is assumed to be a fixed percentage of total length. The length of the fractures represents the propped length. Individual fractures in these simulations are assumed to have a constant fracture conductivity. Shorter fractures are given lower conductivity, under the assumption that they receive less proppant. **Figure 13** shows an example of the simple model, illustrating the more uniform distribution of fracture lengths that are manually input into the model. A heel bias was assumed, with more fluid and longer fractures in the heel clusters of each stage and less fluid and shorter fractures in the toe clusters.

The percentage change in 10-year cumulative oil production is shown in **Figure 14** for the simple and fully coupled models. The zero line is defined by the 10-year production for base-case UIs. The results for both models at the lower range of UIs falls on the same general trend. However, both models show more variation due to well spacing, especially at the high range of UIs. And the variation is different; for example, when UI is 0.9-1 the fully coupled model shows that the improvement in 10-year production decreases as well spacing increases and the simple model shows an opposite trend. The difference in behavior is primarily

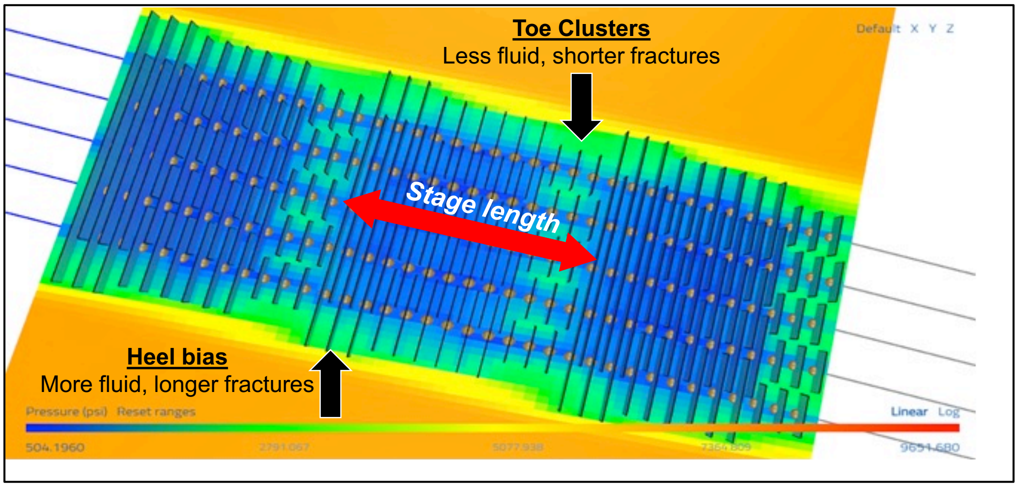

Figure 13 - Example of a simple model.

linked to the degree of heterogeneity in fracture lengths, with relatively uniform fracture lengths in the simple model and a large variation in fracture lengths in the fully coupled model (reference Figure 12 and Figure 13).

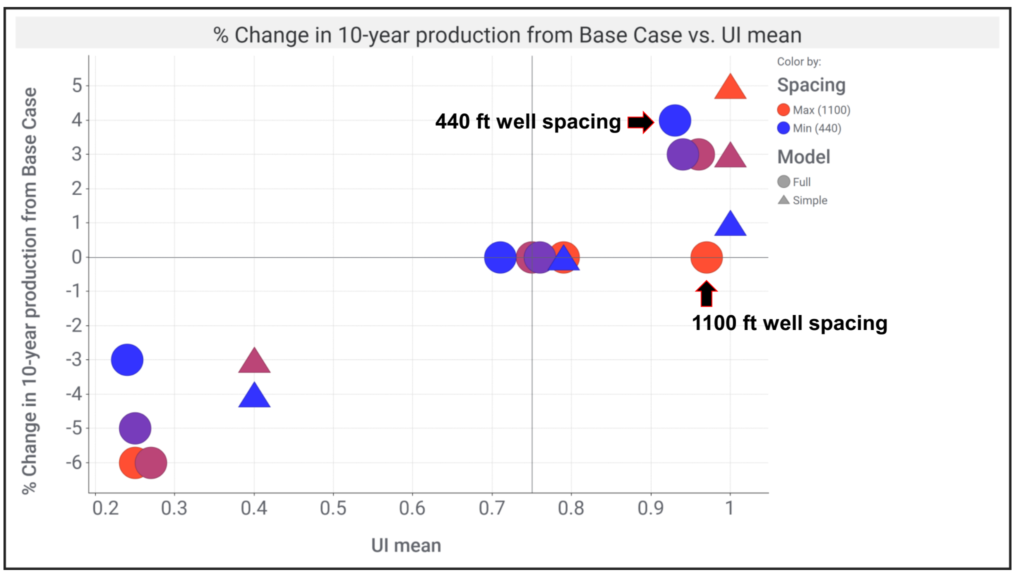

Figure 14 - 10-year production comparison, simple and fully coupled model.

Figure 15 compares the incremental NPV for the two models, showing that the results from the simple model vary dramatically with well spacing. **Figure 16** and **Figure 17** illustrate the drainage differences between the low UI and perfect UI cases for the 440 ft and 1100 ft well spacings, respectively. The results for the fully coupled models using larger well spacing show regions of lower depletion between the wells (see Figure 17) even in the case of the perfect uniformity index driven by stress shadow effects and the resultant fracture shapes. For the 440 ft well spacing, almost the entire area between the wells shows near uniform depletion (Figure 16a), while the low UI case shows significantly more patches of lower depletion. In contrast, for 1100 ft well spacing, even the perfect UI cases shows narrow undepleted channels between the wells (orange colored region between the wells in Figure 17a) as the productive propped length is lower compared to the well spacing. For the Low UI case however, some of the longer fractures can place proppant larger distances which negates the effect of the low UI to some extent.

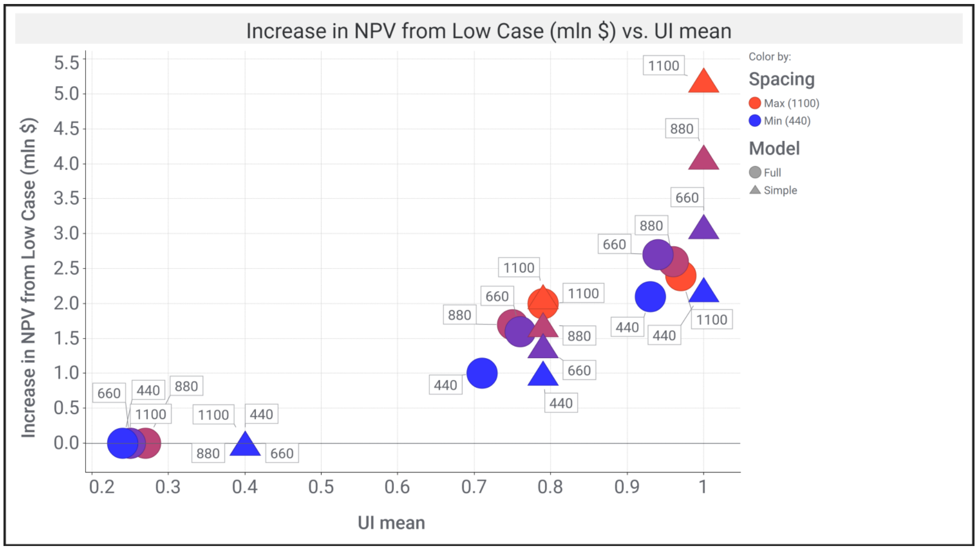

Figure 15 - NPV comparison, simple and fully couple model.

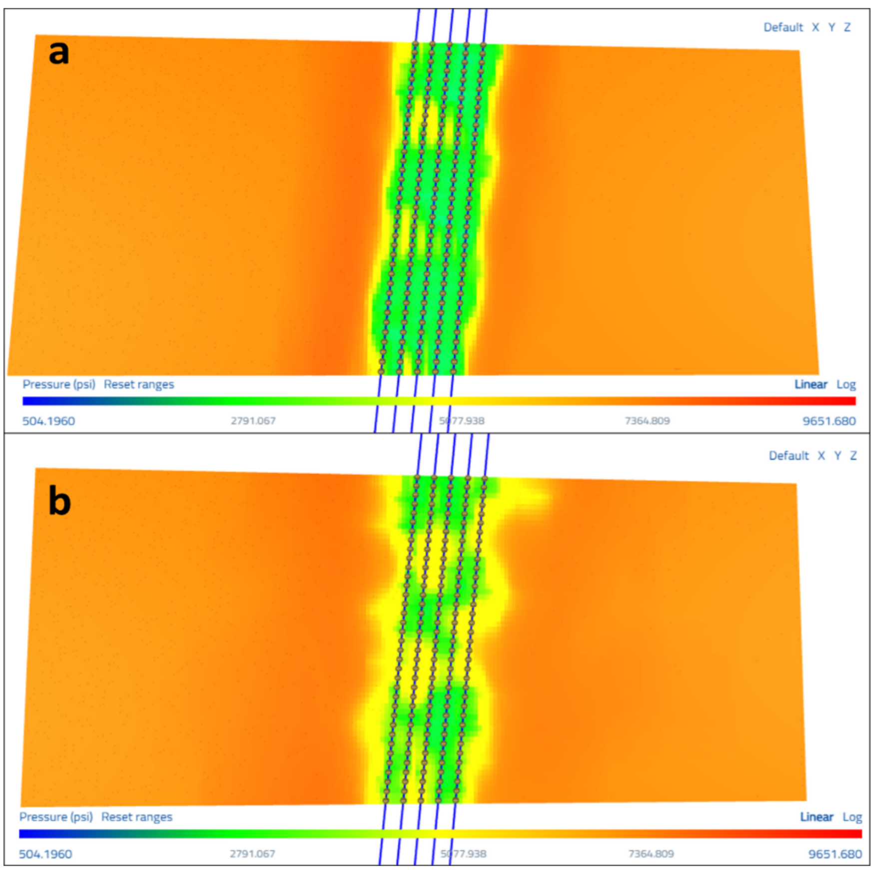

Figure 16 - a) Post-production pressure depletion for a geological layer below the landing zone is shown for 440 ft well spacing in the perfect UI case: b) Pressure depletion for the 440 ft well spacing in the low UI case. Note the higher area covered the yellow patches for the low UI case which leads to sub-optimal drainage.

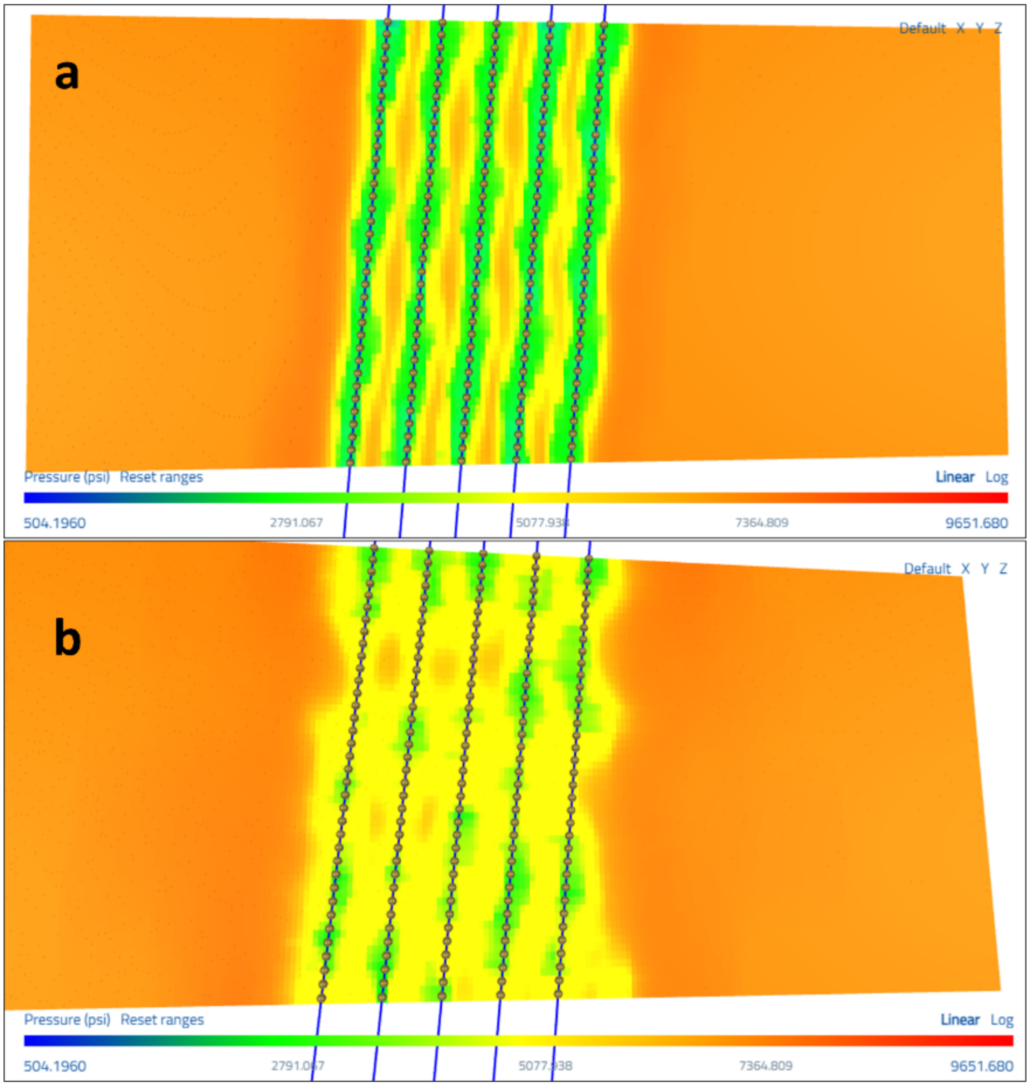

Figure 17 - a) Post-production pressure depletion for a geological layer below the landing zone is shown for 1100 ft well spacing in the perfect UI case. The orange-colored un-depleted regions in between the wells show sub-optimal depletion: b) Pressure depletion for the 1100 ft well spacing in the low UI case. Note the reduction in the orange regions for the Low UI case. This effect is seen more strongly for the baseline UI case.